Balancing Inverted Pendulum Cart on Inclines Using Accelerometers

Cole Woods
Agile Robotics Lab (ARL),
Department of Mechanical Engineering,
University of Alabama,
Tuscaloosa, AL 35406
e-mail: cswoods@crimson.ua.edu

Vishesh Vikas
Agile Robotics Lab (ARL),
Department of Mechanical Engineering,
University of Alabama,
Tuscaloosa, AL 35406
e-mail: vvikas@ua.edu

The balance of inverted pendulum on inclined surfaces is the precursor to their control in unstructured environments. Researchers have devised control algorithms with feedback from contact (encoders—placed at the pendulum joint) and noncontact (gyroscopes, tilt) sensors. We present feedback control of inverted pendulum cart (IPC) on variable inclines using noncontact sensors and a modified error function. The system is in the state of equilibrium when it is not accelerating and not falling over (rotational equilibrium). This is achieved when the pendulum is aligned along the gravity vector. The control feedback is obtained from noncontact sensors comprising a pair of accelerometers placed on the inverted pendulum and one on the cart. The proposed modified error function is composed of the dynamic (nongravity) acceleration of the pendulum and the velocity of the cart. We prove that the system is in equilibrium when the modified error is zero. We present algorithm to calculate the dynamic acceleration and angle of the pendulum, and incline angle using accelerometer readings. Here, the cart velocity and acceleration are assumed to be proportional to the motor angular velocity and acceleration. Thereafter, we perform simulation using noisy sensors to illustrate the balance of IPC on surfaces with unknown inclination angles using proportional-integral-derivative feedback controller with saturated motor torque, including valley profile that resembles a downhill, flat, and uphill combination. The successful control of the system using the proposed modified error function and accelerometer feedback argues for future design of controllers for unstructured and unknown environments using all-accelerometer feedback.
[DOI: 10.1115/1.4052712]

Keywords: control applications, dynamics and control, PID control, robotics, sensors and sensor networks

1 Introduction

The inverted pendulum problem is a classic dynamics and controls problem. The problem generates excitement even among children when they balance a broom in their hand. The feedback received by the child can be characterized as noncontact and contact sensors. Contact sensors are placed at the joint, e.g., encoders (or the child's palm), and are most prevalent due to their simplicity. Noncontact sensors, e.g., gyroscopes, tilt-sensors (child's vision), are also used in tandem for feedback. For example, the JOE robot [1] used a gyroscope to find the angle and angular velocity of the pendulum. Other works have supplemented the encoder feedback with feedback from gyroscopes, accelerometers, tilt-sensor, and vision [2–4]. They have been controlled using multiple techniques that include partial feedback-linearization, geometric proportional-integral-derivative (PID), and Lyapunov-based controllers [5–9]. Application-wise, the wheeled inverted pendulum (WIP), a variant of an inverted pendulum cart (IPC), models self-balancing personal transporters, e.g., segway and unicyle. In addition, the IPC model has also been used as a reduced-order model for human motion [10]. Locomotion and balance of such systems on inclined surfaces require identification of the equilibrium position, hence, the incline angle [2]. Recently, balance of WIP on soft surfaces using full-state feedback PID controllers has been investigated [11].

The equilibrium position of an inverted pendulum is defined as the "dynamic equilibrium axis" that is parallel to the acceleration of the surface of contact [12,13]. This definition explains why we lean forward or backward while sprinting and stopping, align our body along the gravity vector while standing on an incline rather than the surface normal, and the lack of equilibrium position in zero-gravity (space) environments. Accelerometers are noncontact sensors that measure linear acceleration and unlike gyroscopes, they are stable (bias does not drift). They have potential to give feedback that is true to the equilibrium axis and subsequent estimation of the surface incline angle. The challenge for an all-accelerometer arrangement is that it can estimate angular velocity and acceleration, however, cannot differentiate between gravity and dynamic acceleration [14].

Contribution: The research proposes a balance of the IPC using (i) a modified feedback error as cart velocity and dynamic acceleration of the pendulum and (ii) using feedback from noncontact accelerometer sensors—a pair on the pendulum and one on the cart, and motor encoder velocity, and acceleration. In contrast to traditional error functions that comprise system states (five in this case) that need to be controlled, the modified error function is "sensor based" and comprises only three inputs (mean of accelerometers and cart velocity). The zero error implies pendulum alignment with the gravity vector and movement of the cart at a desired velocity. In the process, the accelerometer and motor encoder feedback are able to estimate the angle of the incline and compensate for gravity to determine the dynamic acceleration. In comparison to encoders, the all-accelerometer feedback provide algorithmic and mechanical design advantages. Algorithmically, they facilitate estimation of the incline angle and the modified error function ensures rotational equilibrium. Mechanically, they are noncontact and need not be applied at the cart-pendulum revolute joint.

The rest of this article is structured as follows: Sec. 2 defines the problem and the equilibrium position. Next, Sec. 3 discusses the modified error function. Here, we present the proof of how the system is in equilibrium when the modified error is zero. Thereafter, algorithms for estimating incline and pendulum angle are presented. Section 4 describes the simulation and feedback control

Manuscript received January 25, 2021; final manuscript received October 4, 2021; published online October 26, 2021. Assoc. Editor: Peter H. Meckl.

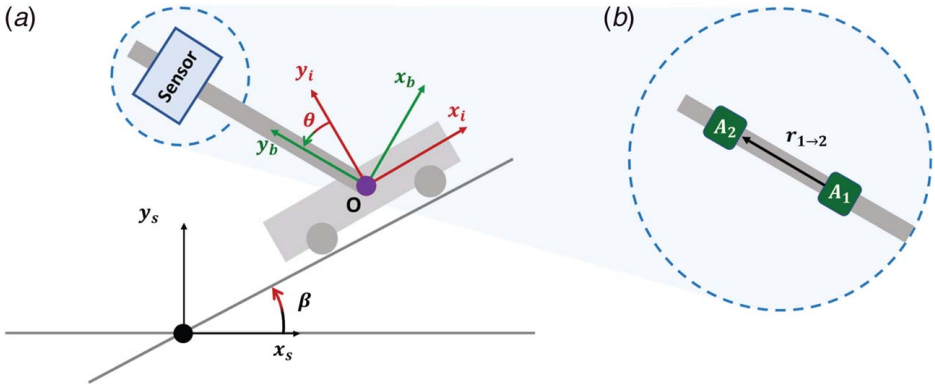

Fig. 1 (*a*) IPC on an incline where the coordinate systems {*s*}, {*i*}, and {*b*} are fixed in the inertial, incline and body reference frames. The angle between {*s*} – {*i*} and {*i*} – {*b*} are the incline angle β, and the pendulum angle θ respectively. Non-contact sensors comprise of one accelerometer A_3 on the cart and (*b*) two accelerometers A_1, A_2 on the inverted pendulum at distances $r_{O\to1}$, $r_{O\to2}$.

details. The results are discussed in the subsequent Sec. 5 before the final conclusion in Sec. 6. The simulation video of the system balancing in variable incline scenario is available online.[1]

2 Problem Definition and Equilibrium Position

Consider an IPC as shown in Fig. 1 where the cart moves on an incline at an angle β. Three coordinate systems are defined - {*s*} to be fixed in the inertial reference frame with origin at the intersection of incline and horizontal with $\{x_s, y_s, z_s\}$ orthonormal basis vectors, {*i*} fixed on the cart reference frame and origin at point *O* with x_i along the incline and z_i out of the plane of the paper, and {*b*} fixed on the pendulum reference frame with origin at *O* and y_b along the pendulum. The cart has mass *M*, and the pendulum has mass *m* with moment of inertia *I* about the center of mass *B* located at distance *l* along the pendulum from point *O*.

Rotation matrices $R_{si} = R_z(\beta)$ and $R_{ib} = R_z(\theta)$ define the relationship between the coordinate systems {*s*}, {*i*} and {*i*}, {*b*}, respectively. $R_z(\alpha) \in \mathbb{R}^{2\times2}$ corresponds to rotation of angle α along axis *z* [15], and s_α, c_α are abbreviations for sin(α), cos(α), respectively.

Subsequently, the kinematics and the kinetic *T* and potential energy *V* of the system are as follows:

$$\begin{aligned} \boldsymbol{r}_O &= x\hat{x}_i, \quad & \boldsymbol{v}_O &= \dot{x}\hat{x}_i \\ \boldsymbol{r}_B &= x\hat{x}_i + l\hat{y}_b, \quad & \boldsymbol{v}_B &= (\dot{x} - lc_\theta\dot{\theta})\hat{x}_i - ls_\theta\dot{\theta}\hat{y}_i \\ & & \omega_{sb} &= \dot{\theta}\hat{z}_s \end{aligned} \tag{1}$$

$$\begin{aligned} T &= \frac{1}{2}m\boldsymbol{v}_O^T\boldsymbol{v}_O + \frac{1}{2}M\boldsymbol{v}_B^T\boldsymbol{v}_B + \frac{1}{2}I\omega_{sb}^T\omega_{sb} \\ &= \frac{1}{2}I\dot{\theta}^2 + \frac{1}{2}M\dot{x}^2 + \frac{1}{2}m(l^2\dot{\theta}^2 - 2lc_\theta\dot{\theta}\dot{x} + \dot{x}^2) \end{aligned} \tag{2}$$

$$\begin{aligned} V &= M\boldsymbol{g}^T(\boldsymbol{r}_O) + m\boldsymbol{g}^T(\boldsymbol{r}_B) \\ &= (M+m)gxs_\beta + mglc_{(\beta+\theta)} \end{aligned} \tag{3}$$

where the gravity $\boldsymbol{g} = g\hat{y}_s = gs_\beta\hat{x}_i + gc_\beta\hat{y}_i$. The following equations of motion are obtained using Lagrangian mechanics, where the Lagrangian $L = T - V$, and *x* and θ are the generalized coordinates

$$\begin{bmatrix} (M+m) & -mlc_\theta \\ -mlc_\theta & (I+ml^2) \end{bmatrix}\begin{bmatrix} \ddot{x} \\ \ddot{\theta} \end{bmatrix} + \begin{bmatrix} ml\dot{\theta}^2 s_\theta + (M+m)gs_\beta + F \\ -mgls_{(\theta+\beta)} \end{bmatrix} = 0 \tag{4}$$

[1] https://youtu.be/K-ABH04Mwp8

Objective and equilibrium position: The objective is to balance the IPC on variable inclined surfaces that have a slope of β such that the pendulum does not fall over and the cart moves at a desired constant velocity. Consequently, the equilibrium position of the system is expressed as follows:

$$\ddot{x}^* = \ddot{\theta}^* = \dot{\theta}^* = 0, \quad \theta^* = -\beta \tag{5}$$

Sensor feedback: The sensor feedback is obtained from the three accelerometers and motor (actuator) encoders.

(1) Pair of accelerometers $\boldsymbol{a}_1, \boldsymbol{a}_2$ placed at $\boldsymbol{r}_{O\to1}, \boldsymbol{r}_{O\to2}$ on the inverted pendulum. Their mean and difference are defined as follows:

$$\begin{aligned} \boldsymbol{a}_d &= \boldsymbol{a}_1 - \boldsymbol{a}_2, \quad & \boldsymbol{r}_d &= \boldsymbol{r}_{O\to1} - \boldsymbol{r}_{O\to2} \\ \boldsymbol{a}_m &= \frac{\boldsymbol{a}_1 + \boldsymbol{a}_2}{2}, \quad & \boldsymbol{r}_m &= \frac{\boldsymbol{r}_{O\to1} + \boldsymbol{r}_{O\to2}}{2} \end{aligned} \tag{6}$$

(2) Accelerometer $\boldsymbol{a}_3$ placed on the cart

$$\boldsymbol{a}_3 = \boldsymbol{a}_O^i = \begin{bmatrix} \ddot{x} \\ 0 \end{bmatrix} + R_{is}\boldsymbol{g}^s, \quad \boldsymbol{g}^s = \begin{bmatrix} 0 \\ g \end{bmatrix} \tag{7}$$

(3) Motor encoder measurements $\dot{\phi}_{motor}$ and $\ddot{\phi}_{motor}$ are assumed to be proportional to the cart speed and acceleration that depend on mechanical parameters, e.g., wheel radius and gear ratio.

$$\dot{x} = K_{\dot{x}}\dot{\phi}_{motor}, \quad \ddot{x} = K_{\dot{x}}\ddot{\phi}_{motor} \tag{8}$$

3 Modified Error Function

For analyzing all-accelerometer feedback, we re-write the acceleration of any point *Q* on the inverted pendulum as follows:

$$\begin{aligned} \boldsymbol{a}_Q^b &= \boldsymbol{a}_O^b + \alpha_{bs}\times\boldsymbol{r}_{O\to Q} + \omega_{bs}\times(\omega_{bs}\times\boldsymbol{r}_{O\to Q}) \\ &= \boldsymbol{a}_O^b + D(\boldsymbol{r}_{O\to Q})\boldsymbol{y} \\ D(\boldsymbol{r}) &= \begin{bmatrix} -r_x & -r_y \\ -r_y & r_x \end{bmatrix} \quad \text{for } \boldsymbol{r} = \begin{bmatrix} r_x \\ r_y \end{bmatrix}, \quad \boldsymbol{y} = \begin{bmatrix} \dot{\theta}^2 \\ \ddot{\theta} \end{bmatrix} \end{aligned} \tag{9}$$

PROPOSITION 1. *For an error function* $\boldsymbol{e}_1 = \boldsymbol{a}_m^S - \boldsymbol{g}^S$, *and* $\ddot{x} = 0$

$$\boldsymbol{e}_1 = 0 \Rightarrow \ddot{\theta} = \dot{\theta} = 0, \quad \theta = -\beta \tag{10}$$

Proof. Using Eqs. (6) and (9), the mean acceleration is expressed as follows:

$$\boldsymbol{a}_m^b = R_{bi}\boldsymbol{a}_O^i + D(\boldsymbol{r}_m)\boldsymbol{y}$$

$$\boldsymbol{a}_O^i = \begin{bmatrix} \ddot{x} \\ 0 \end{bmatrix} + R_{is}\boldsymbol{g}^s$$

$$\Rightarrow \boldsymbol{a}_m^s = R_{sb}\boldsymbol{a}_m^b = R_{si}\boldsymbol{a}_O^i + R_{sb}D(\boldsymbol{r}_m)\boldsymbol{y}$$

$$\Rightarrow \boldsymbol{e}_1 = R_{si}\begin{bmatrix} \ddot{x} \\ 0 \end{bmatrix} + R_{sb}D(\boldsymbol{r}_m)\boldsymbol{y}$$

$$= R_{sb}D(\boldsymbol{r}_m)\boldsymbol{y}, \quad \text{for} \quad \ddot{x} = 0$$

$\boldsymbol{e}_1 = 0 \Rightarrow \boldsymbol{y} = 0 \because |R_{sb}D(\boldsymbol{r}_m)| \neq 0 \Rightarrow \text{rank}(R_{sb}D(\boldsymbol{r}_m)) = 2$. Hence, $\ddot{\theta} = \dot{\theta} = 0$. In addition, using the second row from Eq. (4), it can be deduced that $(\theta + \beta) = 0$ for $\boldsymbol{y} = 0$, $\ddot{x} = 0$. ∎

COROLLARY 1. *For the modified error function* $\boldsymbol{e} = [\dot{x} - \dot{x}_{des}, \boldsymbol{e}_1^T]^T$, *the condition of* $\boldsymbol{e} = 0$ *implies that the IPC is at equilibrium while moving at desired constant velocity of* $\dot{x}_{des}$.

Construction of this modified error requires calculation of the rotation matrix $R_{sb} = R_z(\theta + \beta)$. These angles are obtained by comparing the same vector in two different coordinate systems.

LEMMA 1. *Given a vector* $\boldsymbol{v}$ *representation in {i}, {j}, the angle between the coordinate systems is given by*

$$\phi_{ij} = \text{atan2}\big((\boldsymbol{v}^i \times \boldsymbol{v}^j), (\boldsymbol{v}^i \cdot \boldsymbol{v}^j)\big) \tag{11}$$

$$\text{s.t.} \boldsymbol{v}^i = R_z(\phi_{ij})\boldsymbol{v}^j, \quad \boldsymbol{v}^k = \begin{bmatrix} v_1^k \\ v_2^k \end{bmatrix} \quad \forall k = \{i, j\}$$

$$(\boldsymbol{v}^i \times \boldsymbol{v}^j) = (v_1^i v_2^j - v_2^i v_1^j), \quad (\boldsymbol{v}^i \cdot \boldsymbol{v}^j) = (v_1^i v_2^i + v_1^j v_2^j)$$

where atan2 is the four-quadrant inverse tangent.

Proof. The coordinate systems $\{i\}, \{j\}$ are related by rotation of ϕ_{ij} about z_i axis (out of the plane).

$$\boldsymbol{v}^i = R_z(\phi_{ij})\boldsymbol{v}^j = \begin{bmatrix} c_{\phi_{ij}} & -s_{\phi_{ij}} \\ s_{\phi_{ij}} & c_{\phi_{ij}} \end{bmatrix} \boldsymbol{v}^j$$

$$= \begin{bmatrix} -v_2^j & v_1^j \\ v_1^j & v_2^j \end{bmatrix} \begin{bmatrix} s_{\phi_{ij}} \\ c_{\phi_{ij}} \end{bmatrix}$$

$$\Rightarrow \begin{bmatrix} s_{\phi_{ij}} \\ c_{\phi_{ij}} \end{bmatrix} = \frac{1}{\|\boldsymbol{v}^j\|^2} \begin{bmatrix} -v_2^j & v_1^j \\ v_1^j & v_2^j \end{bmatrix} \begin{bmatrix} v_1^i \\ v_2^i \end{bmatrix}$$

As $\|\boldsymbol{v}^i\|^2 = \|\boldsymbol{v}^j\|^2$, it can be seen that

$$s_{\phi_{ij}} = \frac{(v_1^i v_2^j - v_2^i v_1^j)}{\|\boldsymbol{v}^i\|^2} \quad \text{and} \quad c_{\phi_{ij}} = \frac{(v_1^i v_2^i - v_1^j v_2^j)}{\|\boldsymbol{v}^i\|^2}$$

Geometrically, these are the cross and dot products of the two vectors. The $\|\boldsymbol{v}^i\|^2$ factor can be ignored for the atan2 function as it is a positive nonzero quantity. ∎

3.1 Estimating Pendulum Angle θ

PROPOSITION 2. *The acceleration of the point O in {b} can be calculated using two accelerometers placed on the pendulum* $\boldsymbol{a}_i$ *placed at known displacements* $\boldsymbol{r}_{O\to i}$ *for* $i = 1, 2$.

$$\boldsymbol{a}_O^b = \boldsymbol{a}_m - D(\boldsymbol{r}_m)D(\boldsymbol{r}_d)^{-1}\boldsymbol{a}_d \tag{12}$$

Proof. Using Eqs. (6) and (9), the difference of the accelerometer readings is expressed as follows:

$$\boldsymbol{a}_d = \boldsymbol{a}_1 - \boldsymbol{a}_2 = D(\boldsymbol{r}_d)\boldsymbol{y} \quad \Rightarrow \quad \boldsymbol{y} = D(\boldsymbol{r}_d)^{-1}\boldsymbol{a}_d$$

where $D(\boldsymbol{r})$ is invertible for nonzero $\boldsymbol{r}$. Similarly,

$$\boldsymbol{a}_m = \frac{\boldsymbol{a}_1 + \boldsymbol{a}_2}{2} = \boldsymbol{a}_O^b + D(\boldsymbol{r}_m)\boldsymbol{y}$$

$$\Rightarrow \quad \boldsymbol{a}_O^b = \boldsymbol{a}_m - D(\boldsymbol{r}_m)D(\boldsymbol{r}_d)^{-1}\boldsymbol{a}_d$$ ∎

Hence, using Lemma 1 and Eq. (12),

$$\theta = \text{atan2}\big((\boldsymbol{a}_3 \times \boldsymbol{a}_O^b), (\boldsymbol{a}_3 \cdot \boldsymbol{a}_O^b)\big) \tag{13}$$

3.2 Estimating Incline Angle β.

The accelerometer on the cart measures $\boldsymbol{a}_O^i$

$$\boldsymbol{a}_3 = \begin{bmatrix} a_{3,x} \\ a_{3,y} \end{bmatrix} = \begin{bmatrix} \ddot{x} \\ 0 \end{bmatrix} + \begin{bmatrix} c_\beta & s_\beta \\ -s_\beta & c_\beta \end{bmatrix} \begin{bmatrix} 0 \\ g \end{bmatrix} = \begin{bmatrix} \ddot{x} + g s_\beta \\ g c_\beta \end{bmatrix}$$

Hence, the inclination angle β can be uniquely determined by observing the linear acceleration $\ddot{x}$:

$$\beta = \text{atan2}\big(a_{3,x} - \ddot{x}, a_{3,y}\big) \quad \text{s.t.} \quad \ddot{x} = K_{\ddot{\phi}_{motor}}\ddot{\phi}_{motor} \tag{14}$$

The modified error $\boldsymbol{e}$ is constructed by including the constant desired velocity of the cart $\dot{x}_{des}$, Fig. 2.

$$\boldsymbol{e} = \begin{bmatrix} \dot{x} - \dot{x}_{des} \\ R_z(\theta + \beta)\boldsymbol{a}_m - \boldsymbol{g} \end{bmatrix}, \quad \text{s.t.} \quad \dot{x} = K_{\dot{\phi}}\dot{\phi}_{motor} \tag{15}$$

4 Simulation and Feedback Control

The nonlinear model of the IPC cart, Eq. (4), was simulated in MATLAB®, where the accelerometers were assumed to have white Gaussian noise with power density of $400\,\mu g/\sqrt{\text{Hz}}$ and sampling frequency of 100 Hz, from datasheet of Invensense MPU6050. The other simulation parameters are provided in Table 1, and the gravitational acceleration is assumed to be $g = 9.81$ m/s^2. Motor torque is assumed to be proportional to the force F saturated at ±25 N, and the system is controlled using PI feedback such that

$$F = K_P\boldsymbol{e} + K_I\int \boldsymbol{e}\,dt$$

$$K_P = [43.86\,\text{kg/s}, 43.86\,\text{kg}, 5.86\,\text{kg}]$$

$$K_I = [40.03\,\text{kg/s}^2, 5.04\,\text{kg/s}, 1.04\,\text{kg/s}]$$

The block diagram for the simulation is shown in Fig. 3 where the plant model is constructed using Eq. (4) and accelerometer readings are constructed by adding Gaussian noise to the true signal. Similarly, the modified error generator is shown in Fig. 2.

5 Results and Discussion

We perform simulation to investigate the balancing ability of the IPC (a) using the modified error function and estimation of β on different inclination angles between ±15 deg, (b) for different $\dot{x}_{des}$, and (c) along a terrain similar to a valley (downhill, flat, and then uphill), where the incline angle changes from −15 deg to 0 deg and finally 15 deg. Initial conditions are assumed to be $\dot{\theta}(0) = \theta(0) = \dot{x}(0) = x(0) = 0$.

In the first scenario, the pendulum response is observed for different incline angles β between −15 deg and +15 deg, for $\dot{x}_{des} = 2$ m/s. The system comes to a state of equilibrium, where $\theta = -\beta$, i.e., the pendulum aligns itself along the gravity vector and the dynamic acceleration $\ddot{x}$ is zero, Fig. 4. The system response changes with β and is more desirable (less pendulum oscillation) for declines. The reason why it is easier to balance a pendulum going downhill than it is going uphill is due to the fact that more work must be

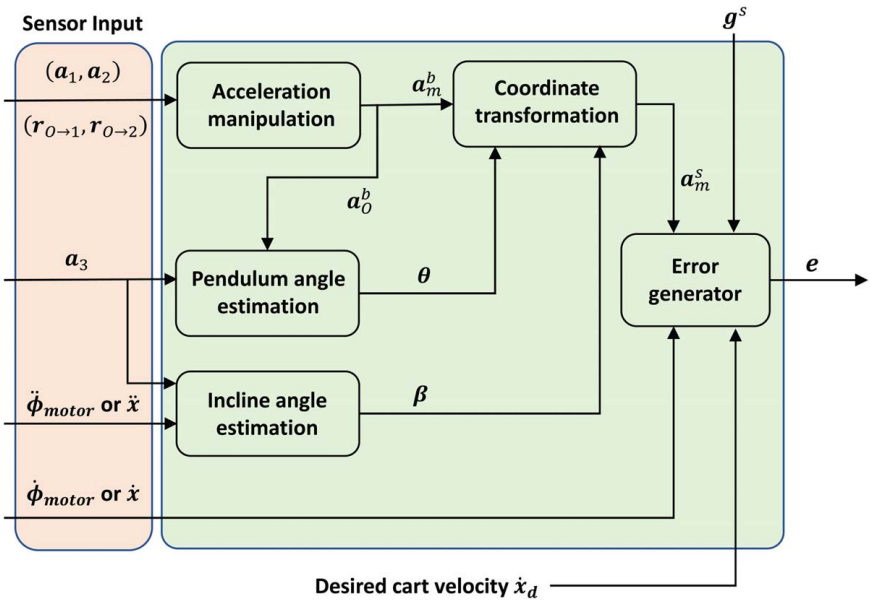

Fig. 2 The modified error is constructed using desired cart velocity $\dot{x}_{des}$ and gravity vector g^S

Table 1 System parameters used in the simulation

M	0.711 kg	m	0.063 kg	l	0.585 m
$r_{O\to1}$	$[0.585, 0]^T$ m	$r_{O\to2}$	$[0.5, 0]^T$ m	I	0.0079 kg/m^2

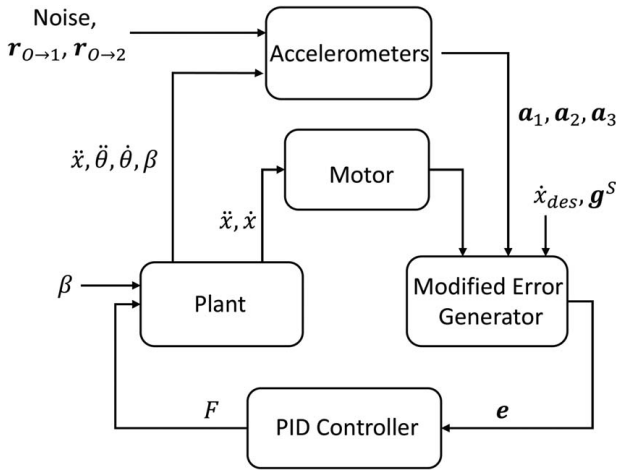

Fig. 3 Block diagram of the SIMULINK® for the system control

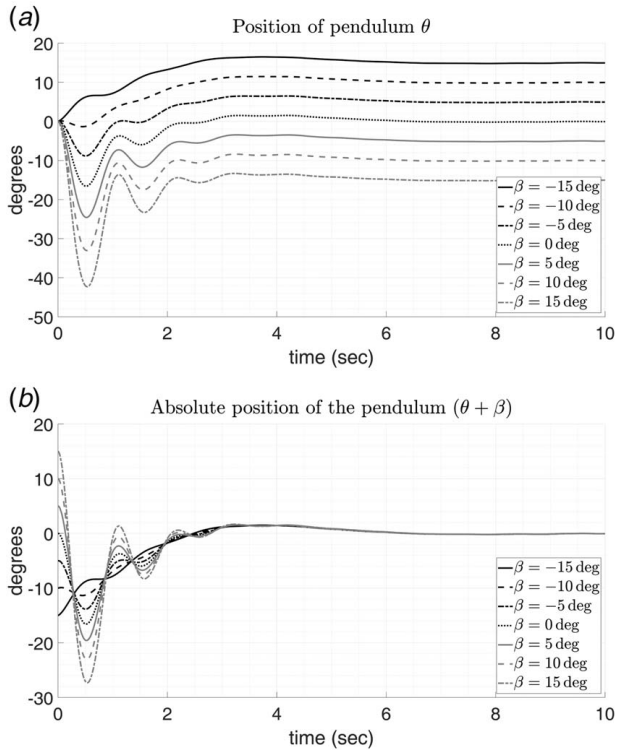

Fig. 4 Position of the pendulum over time with respect to (*a*) the cart θ and (*b*) the inertial coordinate system for $\dot{x}_{des} = 2$ m/s. The plots illustrate the balance of IPC and convergence to the equilibrium angle $\theta = -\beta$.

put into the system that is increasing its potential energy. Integral to this balancing ability is estimation of the incline angle β. Figure 5 illustrates the error in estimation of inclination angle for $\dot{x}_{des} = 2$ m/s. The standard deviation and the maximum error are denoted by σ and max (Δβ). This estimation error occurs during the sudden change in slope as the system accelerates and converges to the true value over time.

In the second scenario, we vary the $\dot{x}_{des}$ between −4 m/s and +4 m/s for $\beta = +15$ deg and observe the absolute position of pendulum, Fig. 6. The system response is symmetric in the sense that the behavior for a given $\dot{x}_{des}$, β is same as that of $-\dot{x}_{des}$, −β, e.g., for the given initial conditions the uphill motion on $\beta = +15$ deg with $\dot{x}_{des} = +4$ m/s will be similar to that of downhill motion with $\dot{x}_{des} = -4$ m/s. Figure 6 also reinforces our intuitive hypothesis that there is an optimal desired velocity for an incline that generates minimal oscillation, e.g., $\dot{x}_{des} = -2$ m/s for the given PI controller on $\beta = +15$ deg. These observations pose questions about design of controllers that minimize system oscillations $(\theta + \beta)$ as $\dot{x}_{des}$ is

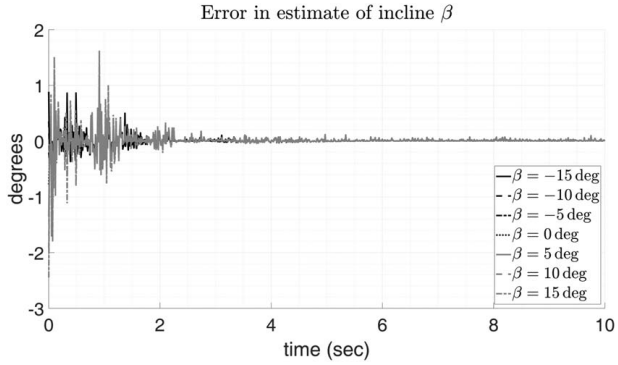

Fig. 5 Error in estimation of β for variable inclines and $\dot{x}_{des} = 2$ m/s. The root-mean-square error (standard deviation) is denoted by σ.

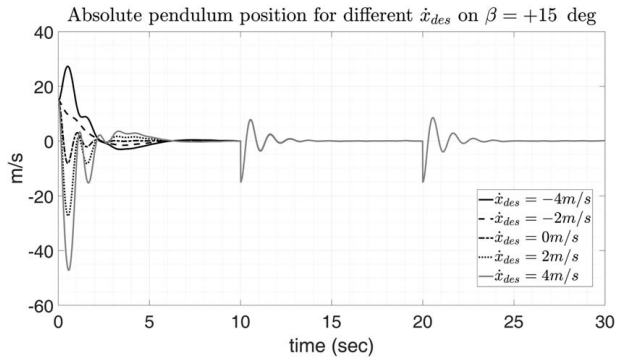

Fig. 6 Absolute position of the pendulum (θ + β) over time as $\dot{x}_{des}$ is varied for β = 15 deg

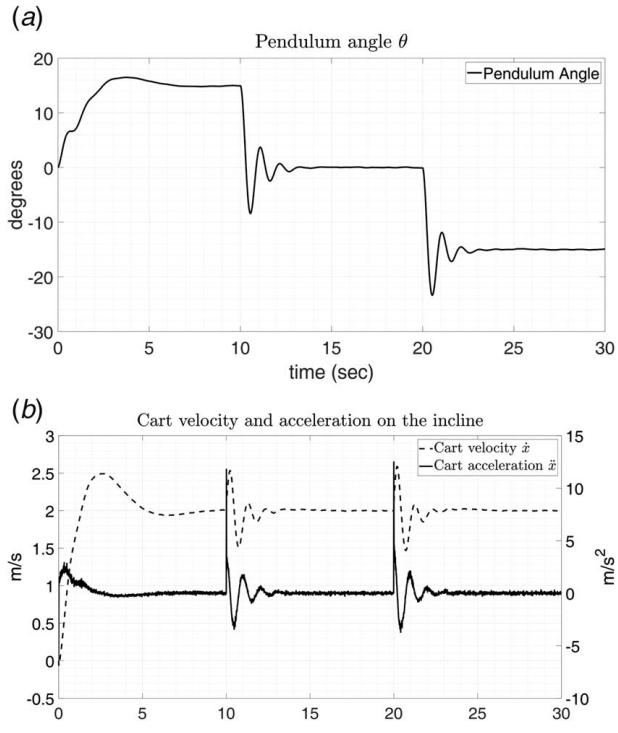

Fig. 7 Balance of IPC on "a valley" where β changes from −15 deg to 0 deg and +15 deg at 10 and 20 s, respectively: (*a*) the pendulum angle adjusts to the sudden change in inclination and (*b*) the cart velocity and acceleration also converge to $\dot{x}_{des}$ = 2 m/s and 0 m/s, respectively

also varied with time as a function of slope β until the final desired value is achieved.

For the final scenario, we simulate the movement of IPC along a valley where the incline angle changes from −15 deg to 0 deg and then +15 deg for $\dot{x}_{des} = 2$ m/s. The incline angle β changes at 10 s and 20 s. The system is able to successfully balance as the incline is suddenly changed. The simulation video of the IPC balancing for this scenario is available online.[2] As the equilibrium state, the system aligns itself along gravity vector θ = −β Fig. 7(*a*), with zero dynamic acceleration and constant velocity, Fig. 7(*b*).

6 Conclusion and Future Work

We presented control of an IPC using feedback from noncontact sensors—a pair of accelerometers located on the pendulum and one on the cart. The proposed modified error function comprises the dynamic acceleration of the pendulum and velocity error of the cart. We proved that when this error was zero, the system does not accelerate and fall over, i.e., aligns itself along the gravity vector. In process, the angle of the incline and the pendulum are estimated using a proposed algorithm where the cart velocity and acceleration are assumed to be proportional to the motor angular velocity and acceleration. The simulation is performed using noisy accelerometers, and the results illustrate that the system balances along different inclines, including a "valley" scenario. This scenario simulates a combination of downhill, flat, and uphill terrain. The system response to variation in desired velocity is investigated and yields encouraging results. These promising results argue for design of accelerometer sensor-based feedback controllers for unstructured and unknown environments where inclines change over time.

Acknowledgment

This research is supported by the National Science Foundation under Grant No. 1832993.

Conflict of Interest

There are no conflicts of interest.

Nomenclature

a_Q^j = acceleration of point Q represented in $\{j\}$ coordinate system
s_α, c_α = abbreviation of sin(α), cos(α) respectively
$\{x_j, y_j, z_j\}$ = orthonormal basis vectors of $\{j\}$ coordinate system
R_{ab} = rotation matrix that transforms vector representation from coordinate system $\{b\}$ to $\{a\}$
$R_z(\alpha)$ = rotation matrix for rotation of angle α about z axis.

$$R_z(\alpha) = \begin{bmatrix} c_\alpha & -s_\alpha \\ s_\alpha & c_\alpha \end{bmatrix}$$

References

[1] Grasser, F., D'Arrigo, A., Colombi, S., and Rufer, A., 2002, "JOE: A Mobile, Inverted Pendulum," IEEE Trans. Ind. Electron., **49**(1), pp. 107–114.
[2] Lee, H., and Jung, S., 2012, "Balancing and Navigation Control of a Mobile Inverted Pendulum Robot Using Sensor Fusion of Low Cost Sensors," Mechatronics, **22**(1), pp. 95–105.
[3] Vasudevan, H., Dollar, A. M., and Morrell, J. B., 2015, "Design for Control of Wheeled Inverted Pendulum Platforms," ASME J. Mech. Rob., **7**(4), p. 041005.
[4] Wang, H., Chamroo, A., Vasseur, C., and Koncar, V., 2008, "Hybrid Control for Vision Based Cart-Inverted Pendulum System," 2008 American Control Conference, Seattle, WA, June 11–13, pp. 3845–3850.
[5] Pathak, K., Franch, J., and Agrawal, S. K., 2005, "Velocity and Position Control of a Wheeled Inverted Pendulum by Partial Feedback Linearization," IEEE Trans. Rob., **21**(3), pp. 505–513.

[2]See Note 1.

[6] Huang, J., Guan, Z., Matsuno, T., Fukuda, T., and Sekiyama, K., 2010, "Sliding-Mode Velocity Control of Mobile-Wheeled Inverted-Pendulum Systems," IEEE Trans. Rob., **26**(4), pp. 750–758.
[7] Maithripala, D. H. S., Madhushani, T. W. U., and Berg, J. M., 2016, "A Geometric PID Control Framework for Mechanical Systems," arXiv:1610.04395.
[8] Maddahi, A., Shamekhi, A. H., and Ghaffari, A., 2015, "A Lyapunov Controller for Self-Balancing Two-Wheeled Vehicles.," Robotica, **33**(1), pp. 225–239.
[9] Ibañez, C. A., Frias, O. G., and Castañón, M. S., 2005, "Lyapunov-Based Controller for the Inverted Pendulum Cart System," Nonlinear Dyn., **40**(4), pp. 367–374.
[10] Kwon, T., and Hodgins, J., 2010, "Control Systems for Human Running Using an Inverted Pendulum Model and a Reference Motion Capture Sequence," Proceedings of the 2010 ACM SIGGRAPH/Eurographics Symposium on Computer Animation, SCA'10, Madrid, Spain, July 2–4, Eurographics Association, pp. 129–138.
[11] Kiselev, O. M., 2020, "Stabilization of the Wheeled Inverted Pendulum on a Soft Surface," arXiv:2006.05450.
[12] Vikas, V., and Crane, C., 2015, "Bioinspired Dynamic Inclination Measurement Using Inertial Sensors," Bioinspirat. Biomimet., **10**(3), p. 036003.
[13] Vikas, V., and Crane, C. D., 2010, "Inclination Estimation and Balance of Robot Using Vestibular Dynamic Inclinometer," IEEE/RAS International Conference on Humanoid Robots, Nashville, TN, Dec. 6–8, pp. 245–250.
[14] Zorn, A., 2002, "A Merging of System Technologies: All-Accelerometer Inertial Navigation and Gravity Gradiometry," Position Location and Navigation Symposium, 2002 IEEE, Palm Springs, CA, Apr. 15–18, IEEE, pp. 66–73.
[15] Murray, R. M., and Sastry, S. S., 1994, *A Mathematical Introduction to Robotic Manipulation*, CRC Press, Boca Raton, FL.